ELSEVIER

Journal of Membrane Science 188 (2001) 87–95

journal of MEMBRANE SCIENCE

www.elsevier.nl/locate/memsci

Preparation and characterization of inorganic hollow fiber membranes

Xiaoyao Tan, Shaomin Liu, K. Li*

Department of Chemical and Environmental Engineering, National University of Singapore, 10 Kent Ridge Crescent, Singapore 119260, Singapore

Received 21 August 2000; accepted 2 February 2001

Abstract

Inorganic hollow fiber membranes were prepared by spinning a polymer solution containing suspended aluminum oxide (Al_2O_3) powders to a hollow fiber precursor, which is then sintered at elevated temperatures. In spinning these hollow fiber precursors, polyethersulfone (PESf), *N*-methyl-2-pyrrolidone (NMP), and polyvinyl pyrrolidone (PVP) were used as a polymer binder, a solvent, and an additive, respectively. The inorganic hollow fiber membranes prepared were characterized using scanning electron microscope (SEM), gas permeation techniques Coulter porometer, and gravimetric analysis. Some primary factors affecting the structure and performance of the membranes such as the sintering temperature and the ratio of the aluminum oxide to the PESf polymer binder were studied extensively. The prepared inorganic membranes show an asymmetric structure, which is similar to the conventional polymeric membranes prepared from the same phase-inversion technique. The inorganic hollow fiber membrane with a higher porosity and better mechanical strength could be prepared by blending the spinning solution with a smaller amount of aluminum oxide powder.

Keywords: Inorganic membrane; Hollow fiber; Preparation

1. Introduction

In the last two decades, membrane technology has been applied commercially to separate individual components from mixtures of liquids and gases. Various polymeric hollow fiber membranes have been prepared and been used widely due to their high surface area per unit volume and high permselectivity. However, the organic materials are only limited to mild operating conditions because of their weak thermal stability and ease of fouling. In contrast, inorganic membranes prepared from microporous glasses, ceramic materials such as aluminum oxide (Al_2O_3), silicon nitride (Si_3N_4), silicon carbide (SiC) [1], metal oxide or metal alloys have relatively high resistance to abrasion and to chemical and thermal degradation, and thus most appropriate for use in severe operating conditions such as corrosive environments and high temperatures. The inorganic membranes are not only used directly in microfiltration, ultrafiltration, and gas separation at high temperatures, but also served as porous supports for dense membrane formation [2]. Microporous Vycor glass, alumina, and some metals are the well-known materials for inorganic membrane production, and numerous studies have been reported for fluid separation or separation/reaction using these inorganic membranes [3–6]. Studies on inorganic

* Corresponding author. Present address: Department of Chemical Engineering, University of Bath, Claverton Down, Bath BA2 7AY, UK. Tel.: +44-1225-826372; fax: +44-1225-826894.
E-mail address: k.li@bath.ac.uk (K. Li).

0376-7388/01/$ – see front matter
PII: S0376-7388(01)00369-6

Nomenclature

B_o	geometric factor of the porous medium (cm^2)
$\bar{d}$	average pore diameter (μm)
d_{max}	maximum pore diameter (μm)
D_o, D_i	outside and inside diameters of the hollow fiber (cm)
L	length of the hollow fiber membrane (cm)
m	mean pore radius of the membrane (μm)
M	molecular weight ($g\,mol^{-1}$)
$\Delta\bar{p} = (p_1 + p_2)/2$	mean pressure (p_1 and p_2 are the upstream and downstream pressures) ($dyn\,cm^{-2}$)
P	permeability coefficient ($cm^2\,s^{-1}$)
P_o	Knudsen permeability coefficient ($cm^2\,s^{-1}$)
q	tortuosity factor
R	gas constant ($R = 8.3174\,m^3\,Pa\,mol^{-1}\,K^{-1}$)
T	absolute temperature (K)
w_{wet}	weight of the wet fiber sample (g)
w_{dry}	weight of the dry fiber sample (g)
w_T	total weight of Al_2O_3 powders used for spinning of fibers (g)
$w_{0.01}$	weight of the 0.01 μm Al_2O_3 powder (g)

Greek letters

δ	membrane thickness (cm)
ε	surface porosity
ε_v	volumetric porosity of the hollow fiber membrane
η	viscosity of the permeant ($dyn\,s\,cm^{-2}$)
ρ_{H_2O}	density of deionized water ($g\,cm^{-3}$)

membranes, especially inorganic hollow fiber membranes, prepared from other materials are relatively scarce partly because their production processes are complicated and are too expensive.

There are many different methods used for preparing inorganic hollow fibers, including dry spinning a system of inorganic material and binder [1], wet spinning a suitable inorganic material-containing solution and/or sols [7], depositing fibers from the gas phase on to a substrate, or pyrolyzing the polymers [8–10]. In this study, we have attempted to use the well-known phase-inversion method, commonly employed for spinning polymeric hollow fiber membranes, to prepare the inorganic Al_2O_3 hollow fibers. Factors affecting the structure and performance of the membranes such as the sintering temperature and the ratio of the aluminum oxide to the polyethersulfone (PESf) polymer binder were studied extensively, and the formation procedures of the inorganic hollow fiber membrane were also discussed.

2. Experimental

2.1. Materials

Commercially available Al_2O_3 powders with two different particle diameters of 0.01 (gamma/alpha, 99.98% metal basis) and 1 μm (alpha, 99.9% metal basis) (purchased from Alfa AESAR, A Johnson Matthey Company) were used as the membrane materials. PESf (Radel A-300, Ameco Performance, USA) and *N*-methyl-2-pyrrolidone (NMP) (Synthesis Grade, Merck) were used to prepare the polymer solution. Polyvinylpyrrolidone (PVP, K90) (GAF® ISP Technologies, Inc., M_w = 630,000) was used as an additive. Tap water (Public Utility Board (PUB), Singapore) was used as both the internal and external coagulants.

2.2. Preparation of spinning dope

The required quantity of NMP was taken in one-liter wide-neck reaction flask and the PESf was slowly added over a period of 30 min to form the polymer solution. After the polymer solution was formed, a given amount of aluminum oxide (1 μm or a mixture of 1 μm and 0.01 μm) was then added into the polymer solution slowly, while Heidolph RZR 2000 stirrer was used at a speed of ∼300 rpm to ensure that all the aluminum oxide powders is dispersed uniformly in the polymer solution. PVP as an additive was also introduced into the solution to modulate its viscosity. Finally, the polymer solution was degassed at the room temperature.

Table 1
Hollow fiber precursor spinning conditions

Spinning parameters	
Dope composition (wt.%)	
Al_2O_3 (1 μm)	50–57.7
Al_2O_3 (0.01 μm)	0–2.9
PESf, Radel A-300	6.4–10
NMP	35–40
PVP K-90	0.5–0.9
Dope temperature (°C)	27
Coagulation bath temperature (°C)	27
Internal coagulant temperature (°C)	27
Injection rate of internal coagulant (ml min^{-1})	3
Nitrogen pressure (psi)	20–30
Air gap (cm)	2
Linear extrusion speed (m min^{-1})	5

2.3. Fabrication of inorganic hollow fiber membranes

The degassed dope containing the dispersed aluminum oxide powders was transferred to a stainless steel reservoir and pressurized to 20–30 psig using nitrogen. A tube-in-orifice spinneret with orifice diameter/inner diameter of the tube of 2.0/0.72 (mm) was used to obtain hollow fiber precursors. The air gap was kept at 2 cm for all spinning runs. Finally, the forming hollow fiber precursor was passed through a water bath to complete the solidification process and thoroughly washed in water. The details of the spinning equipment and procedure on hollow fiber spinning have been described elsewhere [11]. Table 1 shows the spinning conditions employed in this study.

The hollow fiber precursors were first heated in the carbolite furnace at about 500°C for 2 h to remove the organic polymer binder, and then were calcined at a high temperature for about 5 h to allow the fusion and bonding to occur. The calcination temperature used in this study was between 1180 and 1600°C.

2.4. Scanning electron microscopy (SEM)

Structures of the prepared hollow fiber membranes were visually observed using a scanning electron microscope (Hitachi Model S-4100). The precursor hollow fiber was first immersed in liquid nitrogen. After about 10 min, the frozen membranes were slowly flexed in the liquid nitrogen until a clear cross-sectional fracture occurred. For the inorganic hollow fiber (after calcination), the clear cross-sectional fracture may be obtained by directly snapping the fiber. These membrane samples were then positioned on a metal holder and gold-coated using sputter-coating operated under vacuum. The SEM micrographs of both surface and cross-section of the hollow fiber membranes were taken at various magnifications.

2.5. Gas permeation study

The mean pore size and the effective surface porosity of the inorganic hollow fiber membranes prepared were determined using the gas permeation method suggested by Yasuda and Tsai [12]. The gas permeability coefficient ($cm^2\ s^{-1}$), P, of a porous medium may be expressed as [13]

$$P = P_o + \left(\frac{B_o}{\eta}\right)\Delta\bar{p} \tag{1}$$

where $\Delta\bar{p} = (p_1 + p_2)/2$ (p_1 and p_2 are the upstream and downstream pressures (dyn cm^{-2}), respectively), P_o the Knudsen permeability coefficient ($cm^2\ s^{-1}$), B_o the geometric factor of the porous medium (cm^2), and η the viscosity of the permeant (dyn s cm^{-2}).

Values of P_o and B_o can be obtained from the data of P as a function of $\Delta\bar{p}$. The mean pore radius (cm), m, and the effective surface porosity, ε/q^2, can be determined from the following equations [13,14]:

$$m = \frac{B_o}{P_o}\frac{16}{3}\sqrt{\frac{2RT}{\pi M}} \tag{2}$$

where

$$P_o = \frac{4}{3}\sqrt{\frac{8RT}{\pi M}}\frac{\delta\varepsilon m}{k_1 q^2} \tag{3}$$

$$B_o = \frac{\varepsilon m^2}{kq^2} \tag{4}$$

where $\delta/k_1 = 0.8$ and $k = 2.5$ are assumed for all the membranes [13,14], q the tortuosity factor, and ε the porosity.

Purified nitrogen was used as the test gas for the measurements of the permeability coefficient, P, of the inorganic hollow fibers prepared. The results were then used for calculation of the mean pore radius,

Table 2
Experimental results

Number	Al_2O_3/PESf	Sintering temperature (°C)	Al_2O_3 particles used (1 μm/0.01 μm)	Pore size		Porosity	
				d_{max} (μm)	$\bar{d}$ (μm)	$\varepsilon/q^2 \times 10^2$	ε_v
1	5	1600	100/0	0.257	0.106	0.339	0.266
2	8	1600	100/0	0.162	0.067	0.242	–
3	9	1600	100/0	0.132	0.056	0.194	–
4	5	1180	100/0	0.521	0.130	0.647	0.488
5	5	1400	100/0	0.306	0.097	0.513	0.427
6	5	1500	100/0	0.275	0.114	0.393	0.285
7	8	1550	100/0	0.187	0.040	0.037	0.062
8	8	1550	97/3	0.152	0.043	0.081	0.096
9	8	1550	95/5	0.113	0.048	0.155	0.133

m, and the effective surface porosity, ε/q^2, using the above-mentioned equations (Eqs. (1)–(4)). Both the calculated mean pore diameter, $\bar{d} = 2m$, and the effective surface porosity, ε/q^2, are given in Table 2.

2.6. Determination of volumetric porosity and maximum pore size

Volumetric porosities of the inorganic hollow fiber membranes were determined based on the gravimetric analysis of water entrapped in the pores of the fiber walls. The inorganic hollow fibers with length L were first wetted by immersing it in deionized water, and the weight of the wet fibers was then measured. The weight of the dry fibers was also measured after the entrapped water was completely removed by drying the wet fiber in an oven at 250°C for 5 h. The volumetric porosity, ε_v, was calculated from the following equation:

$$\varepsilon_v = \frac{(w_{wet} - w_{dry})/\rho_{H_2O}}{(1/4)\pi L(D_o^2 - D_i^2)} \quad (5)$$

where w_{wet}, w_{dry}, ρ_{H_2O}, and ε_v are the weights of the wet and dry fiber samples, the density of deionized water, and the volumetric porosity of the hollow fiber, respectively.

The maximum pore size of the hollow fiber membrane was measured using Coulter porometer manufactured by Coulter Electronics Ltd, UK. The values of the volumetric porosity, ε_v determined above and maximum pore size, d_{max}, measured for the inorganic hollow fiber membranes prepared at different conditions are also listed in Table 2.

3. Results and discussion

3.1. Morphology study of aluminum oxide hollow fiber membranes

SEM micrographs of the hollow fiber precursor and its sintered fiber, spun from the dope-containing Al_2O_3 (1 μm) 50%, PESf 10%, PVP 0.5%, and NMP 39.5%, and coagulated in water bath at room temperature, are shown in Figs. 1 and 2, respectively. It can be seen from the micrograph of Fig. 1(a) that the o.d. and i.d. of the fiber precursor prepared were measured to be 1287 and 847 μm, respectively. The micrograph of Fig. 1(b) illustrates that near the outer and inner walls of the fiber precursor, long finger-like structures are present and that at the center of the hollow fiber precursor, sponge-like structures are possessed. The appearance of the fiber structures shown in Fig. 1 can be attributed to the rapid precipitation which occurred at both the inner and outer fiber walls, resulting in long fingers and slow precipitation giving the sponge-like structure at the center of the fiber. Micrograph of Fig. 1(c) shows the surface of the hollow fiber precursor. It can be seen that the surface of the precursor is similar to the conventional polymeric membranes prepared via the phase-inversion technique.

Fig. 2 shows the micrographs of the sintered hollow fiber. The sintering process was carried out in air at a temperature of 1500°C. It can be seen from the micrograph of Fig. 2(a) that the o.d. and i.d. of the sintered fiber were shrunk from 1287 and 847 μm to 1044 and 726 μm, respectively. The cross-sectional structure of the sintered fiber as shown in Fig. 2(b) is the same

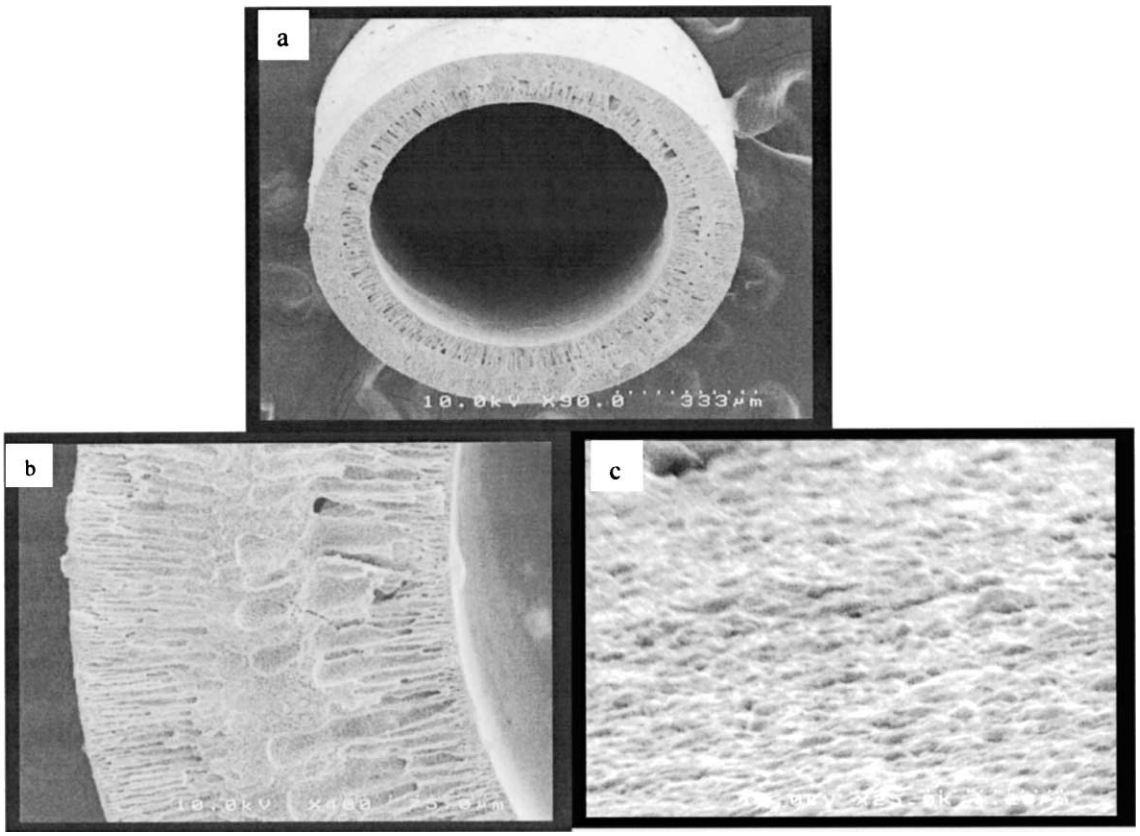

Fig. 1. SEM diagrams of the hollow fiber before sintering: (a) cross-section; (b) membrane wall; (c) membrane surface.

as that of the precursor, i.e. the sponge-like structures at the center are sandwiched by the long finger-like structures located at the outer and inner walls of the fiber. Further comparing the SEM photos, especially for the surfaces between the precursor (Fig. 1(c)) and the sintered fiber (Fig. 2(c)) reveals that the pore quantity and pore size may have changed after the sintering process, although the general structure is maintained. Such structure changes depend on the composition of the dope solution and the sintering temperature, which are discussed and presented in Section 3.2.

3.2. Effect of aluminum oxide content

The hollow fiber precursor formed through the phase-inversion technique contains the Al_2O_3 and the PESf polymer. During the sintering process, the PESf is removed and the Al_2O_3 hollow fiber is ultimately formed. Therefore, the Al_2O_3 content in the spinning dopes plays an important role in determining the pore size and porosity of the fiber formed. The structure parameters such as pore size and surface porosity of the hollow fibers were, therefore, studied with different Al_2O_3/PESf ratios. The results are shown in Fig. 3. All the fiber samples were sintered at a temperature of 1600°C. As shown in Fig. 3, both the pore size and the surface porosity decrease as the Al_2O_3/PESf ratio is increased. This indicates that in order to produce the denser membrane, the higher Al_2O_3 content in the solution dope must be maintained. However, our experimental results revealed that it is difficult to form a hollow fiber precursor if the Al_2O_3/PESf ratio is greater than 9.

3.3. Effect of sintering temperature

Experimental results for this effect are given in Fig. 4. The fiber precursors used in the sintering

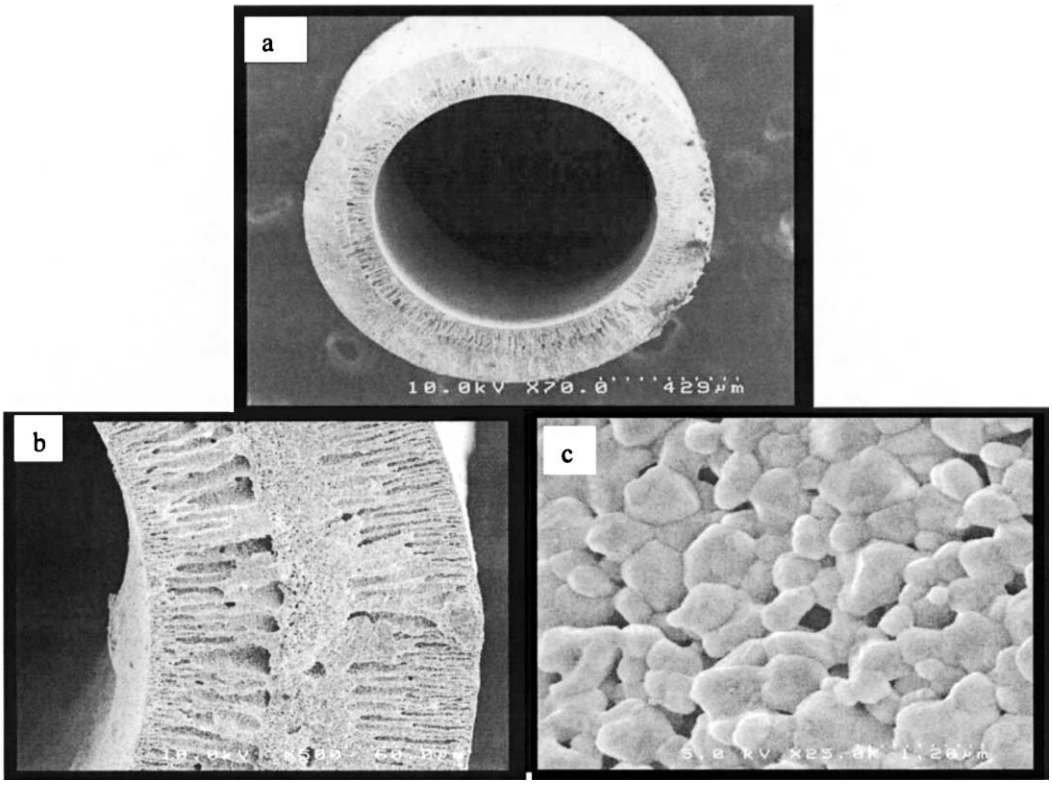

Fig. 2. SEM diagrams of the hollow fiber after sintering: (a) cross-section; (b) membrane wall; (c) membrane surface.

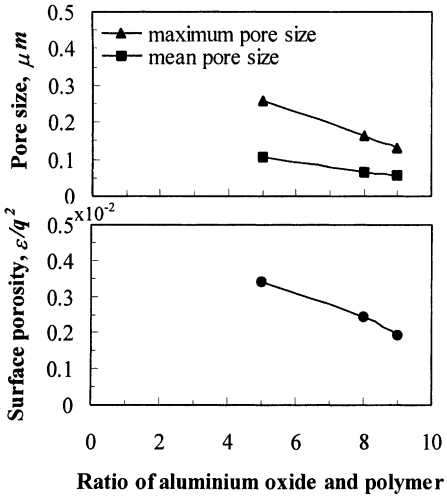

Fig. 3. Effect of aluminum oxide content on the membrane surface structure.

process were prepared from the solution dope containing the same composition (Al_2O_3/PESf ratio 5:1). Therefore, the change of structure of the final hollow fibers is only due to the sintering temperature. As can be seen in Fig. 4, the maximum pore size, likely the defect pores, decreases as the sintering temperature is increased. The change of average pore size with the temperature is, however, negligible.

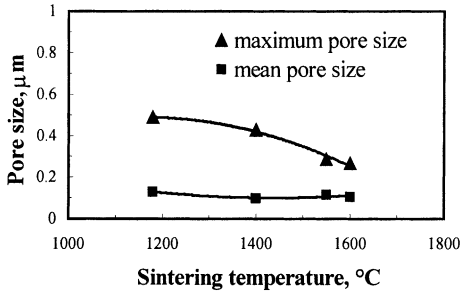

Fig. 4. Effect of sintering temperature on the membrane pore size.

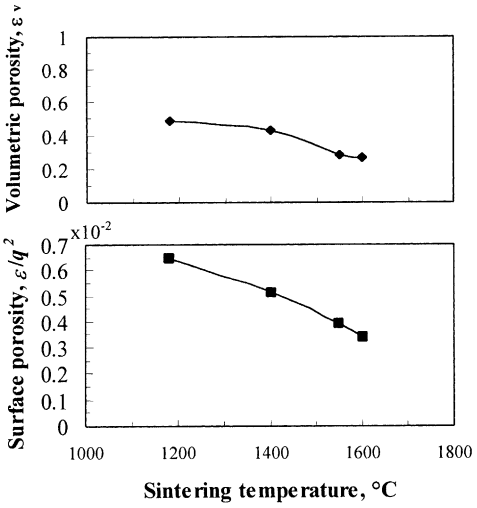

Fig. 5. Effect of sintering temperature on the membrane porosity.

Membrane shrinkage was observed after the sintering process, the extent of which increases with the sintering temperature. The shrinkage ratio, defined as the ratio of the sintered fiber o.d. to the fiber precursor o.d., was found to be decreased from about 0.932 to 0.739 when the sintering temperature was increased from 1180 to 1600°C. The decrease in the maximum pore size is possibly due to such shrinkage. As for the average pore size, the phenomenon of the negligible temperature effect may be explained by the Rhines' topological decay model [15]. During the sintering process, the pore network formed by many nodes and channels decays in a stable manner. The ratio of the pore volume fraction to the pore surface area, however, remains unchanged [15]. Since the channel radius is proportional to this ratio, it must also remain as a constant. Thus, as the sintering temperature increases, densification of the fiber is proceeded by a reduction of the total length and number of channels, and the pore diameters however remain unchanged. Such a phenomenon was also observed by Page and Pan [16].

Although, increasing the sintering temperature favors the uniformity of the membrane pore, unfortunately, both the volumetric porosity and the surface porosity decreases with increase in the sintering temperature, as shown in Fig. 5. This implies that the pore blockage instead of the pore expansion predominates the change of the membrane structure. Nevertheless, the occurrence of fusion and bonding at high temperature is essential to the fiber formation. In fact, the alumina hollow fibers with great mechanical strength could not be prepared unless the sintering temperature is increased to 1500°C.

3.4. Effect of particle size

Size of the Al_2O_3 particles plays an important role in fabricating a desired Al_2O_3 hollow fiber. It has been found that smaller pores and substantial flaw-free membranes could be produced when a smaller particle diameter is employed [17]. However, in this study, difficulties of using 0.01 μm Al_2O_3 particles for preparing the inorganic hollow fibers were experienced. An Al_2O_3 paste instead of the dope solution was formed during the formation of the spinning dope using the 0.01 μm particles alone even at a very low Al_2O_3/PESf ratio. This is probably due to the large surface area of the small particles resulting in less fluidity of the dope solution. Therefore, the Al_2O_3 hollow fiber was not able to spin from the 0.01 μm particles alone; instead, the 0.01 μm particles were blended in the 1 μm particle solutions used above for spinning of the Al_2O_3 hollow fibers.

Fig. 6 shows the effect of the weight percent, i.e. 0.01 μm particles, $w_{0.01}$ over total Al_2O_3 particles, w_T ($w_{0.01}/w_T$, %), on the pore size of the resulting hollow fibers. All the samples were sintered at 1550°C from precursors spun from the dope solution with the ratio of Al_2O_3/PESf of 8. It can be seen that the maximum pore size decreases as the content of 0.01 μm Al_2O_3 particles is increased, however the reverse is observed for the average pore size. This suggests that the pores of the hollow fibers prepared may be more

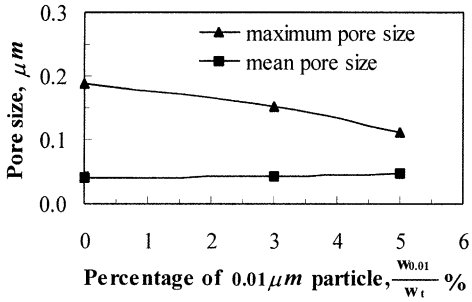

Fig. 6. Effect of content of the 0.01 μm Al_2O_3 particles on the membrane pore size.

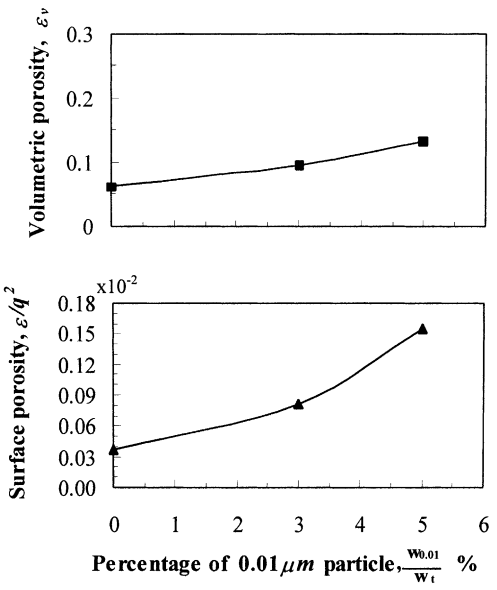

Fig. 7. Effect of content of the 0.01 μm Al_2O_3 particles on the membrane porosity.

uniform in size by adding the 0.01 μm particles in the spinning solutions.

The effect of the weight percent of the 0.01 μm particles on porosities of the resulting hollow fibers is illustrated in Fig. 7. It can be seen that both the surface and the volumetric porosities increase as the content of the 0.01 μm particles is increased. This result is contrary to the analysis conducted by Lu [18], who showed theoretically that the porosity of a ceramic powder compact reduces when smaller particles are used alone for preparation of the powder compact. In this study, a phase-inversion process was employed for spinning of the hollow fiber. As pore formers were added into the spinning dope, asymmetric structure and surface pores of the fiber precursor were formed during the coagulation process and were altered after the sintering. In view of the complicity of the combined spinning and sintering processes, the relationship between the powder size and the structure of the final resulting membrane remains unclear and need to be further explored. The presence of the 0.01 μm particles, however, enhances significantly the mechanical strength of the hollow fibers. Unfortunately, it was observed that the dope solution would turn to a paste again, once the content of the 0.01 μm particles in the total alumina powders is greater than 5%.

4. Conclusions

Inorganic hollow fiber membranes have been prepared by spinning a polymer solution containing suspended Al_2O_3 powders to a hollow fiber precursor, which is then sintered at elevated temperatures. The prepared membranes have the asymmetric structure including the sponge-like structures at center, sandwiched by the long finger-like structures located at the outer and inner walls of the fiber.

The experimental results obtained from the permeation study indicate that as the Al_2O_3/PESf ratio is increased, both the pore size and porosity of the resulting membrane decrease. In order to prepare a solution dope, which is suitable for the spinning process, the value of the Al_2O_3/PESf ratio must be controlled at 9 or less.

It was found that the maximum pore size of the inorganic membrane prepared decreases as the sintering temperature is increased. The change of average pore size with the temperature is, however, negligible. Uniformity of pores and porosities of the inorganic hollow fiber membrane could be improved significantly by blending some of the 0.01 μm Al_2O_3 powders into the forming dopes. More importantly, the addition of the fine particles enhances considerably the mechanical strength of the resulting hollow fiber, which is essential to its practical use in various fluid separations.

Acknowledgements

The authors gratefully acknowledge the research funding (RP3972690) provided by the NUS. A research scholarship provided by National University of Singapore to one of the authors, Liu Shaomin, is also gratefully acknowledged.

References

[1] R.A. Terpstra, J.P.G.M. Van Eijk, F.K. Feenstra, Method for the production of ceramic hollow fibers, US Patent No. 5,707,584 (1998).

[2] J.J. Hammel, Porous inorganic siliceous-containing gas enriching material and process of manufacture and use, US Patent No. 4,853,001 (1989).

[3] J.D. Way, D.L. Roberts, Hollow fiber inorganic membrane for gas separations, Sep. Sci. Technol. 27 (1992) 29.

[4] M. Bhandarkar, A.B. Shelekhin, A.G. Dixon, Y.H. Ma, Adsorption, permeation and diffusion of gases in microporous membranes. 1. Adsorption of gases on microporous glass membranes, J. Membrane Sci. 75 (1992) 221.
[5] V. Shindo, T. Hakuta, H. Yoeshitome, H. Inouei, Gas diffusion in microporous media in Knudsen's regime, J. Chem. Eng. Jpn. 16 (1983) 120.
[6] H.P. Hsieh, Inorganic membrane reactors, Catal. Rev.-Sci. Eng. 33 (1/2) (1991) 1.
[7] K.H. Lee, Y.M. Kim, Asymmetric hollow inorganic membranes, Key Eng. Mater. 61/62 (1991) 17.
[8] J.E. Koresh, A. Sofer, Molecular sieve carbon permselective membrane. Part I. Presentation of a new device for gas mixture separation, Sep. Sci. Technol. 18 (1983) 723.
[9] J.E. Koresh, A. Sofer, Mechanism of permeation through molecular-sieve carbon membrane, J. Chem. Soc., Faraday Trans. 82 (1986) 2057.
[10] V.M. Linkov, R.D. Sanderson, E.P. Jacobs, Highly asymmetrical carbon membranes, in: Proceedings of the 34th IUPAC Symposium on Macromolecules, Vol. 7, 1992, p. 56.
[11] S.P. Deshmukh, K. Li, Effect of ethanol composition in water coagulation bath on morphology of PVDF hollow fiber membranes, J. Membr. Sci. 150 (1998) 75.
[12] H. Yasuda, J.T. Tsai, Pore size of microporous polymer membranes, J. Appl. Polym. Sci. 18 (1974) 805.
[13] P.C. Carman, Flow of Gases through Porous Medium, Butterworths, London, 1956 (Chapters 1 and 3).
[14] I. Cabasso, K.Q. Robert, E. Klein, J.K. Smith, Porosity and pore size determination in polysulfone hollow fibers, J. Appl. Polym. Sci. 21 (1977) 1883.
[15] F.N. Rhines, R.T. Dehoff, Channel network decay in sintering, Mater. Sci. Res. 16 (1984) 49.
[16] R.A. Page, Y.M. Pan, Microstructure evolution during sintering, Mater. Res. Soc. Symp. Proc. 249 (1992) 449.
[17] E.J. DoBo, Process to produce inorganic hollow fibers, US Patent No. 4,222,977 (1980).
[18] G.Q. Lu, Evolution of the pore structure of a ceramic powder compact during sintering, J. Mater. Process Tech. 59 (1996) 297.